





Effect of Changing Environment on the Dynamic Characteristics of an Overpass

Carmelo Gentile^(✉) , Marco Pirrò , and Fulvio Busatta

DABC, Politecnico di Milano, P.Za Leonardo da Vinci 32, 20133 Milan, Italy
carmelo.gentile@polimi.it

Abstract. Selected results collected in the continuous dynamic monitoring of a 3-span overpass using MEMS accelerometers are reported in the paper. The investigated structure is a steel-concrete composite bridge characterized by a rather complex geometry. The overpass has a total length of 108 m and spans of 30 m + 48 m + 30 m.

Several bending and torsion modes are identified during the continuous monitoring, with the temperature significantly affecting all natural frequencies. Moreover, a clear effect of changing environment is detected for torsion modes as well, whereas no remarkable changes of bending mode shapes are detected.

Keywords: Bridge · Environmental effects · Operational Modal Analysis · Structural Health Monitoring

1 Introduction

In the last few years, the Structural Health Monitoring (SHM) strategy based on vibration monitoring and operational modal analysis (OMA, i.e. the output-only identification of modal parameters) has received increasing attention in the field of Civil Engineering structures and many dynamic monitoring systems have been installed especially in bridges [1], all over the world. Well-known examples of permanently monitored bridges in different countries include the Z24 bridge [2] in Switzerland, the Infante D. Enrique bridge [3] in Portugal, the Tamar bridge [4] in South-west England, the San Michele bridge [5] and the Brivio bridge [6] in Italy.

The detection of structural anomalies is often performed by applying the Statistical Pattern Recognition (SPR) paradigm [7] to continuously identified modal parameters [3]. Since the modal parameters (and especially natural frequencies) are also affected by environmental and operational variability (EOV) [2–6], the main objective of SPR approaches is to distinguish the patterns of variations associated to normal EOV from the ones associated to damaged conditions. Hence, the Cointegration technique [8, 9] and the Modal Assurance Criterion (MAC) [10] might be adopted to identify abnormal changes in natural frequencies and mode shapes, respectively.

The present paper is mainly aimed at presenting selected results from the dynamic monitoring of a steel-concrete composite overpass. After a concise description of the bridge, the dynamic characteristics of the overpass are presented and compared with

the predictions obtained using a 3D finite element (FE) model of the structure. The second part of the paper focuses on the continuous dynamic monitoring of the bridge and the influence of environmental parameters on the variations observed in both natural frequencies and (torsion) mode shapes.

2 Description of the Investigated Bridge

The investigated bridge (Fig. 1), denoted to as *Dolo* Overpass in the following, is a steel-concrete composite bridge that crosses the A4 Milan-Venice highway in the municipality of Dolo (VE). The infrastructure has an overall length of 108 m (Figs. 1 and 2) and consists of three spans of different lengths: the largest span, crossing the A4, is 48 m long whereas the length of side-spans is 30 m.

The total width of the deck is 15.4 m for two traffic lanes of 12 m and two pedestrian walkways. The cross-section of the bridge (Fig. 1b) consists of a trapezoidal steel box girder framed by equally spaced steel cross-beams; the girder and the cross-beams exhibit variable height and are composite with a r.c. slab.

As shown in Fig. 1a, the central span is supported by elastic constraints made of inclined steel struts resting on squat r.c. piers.

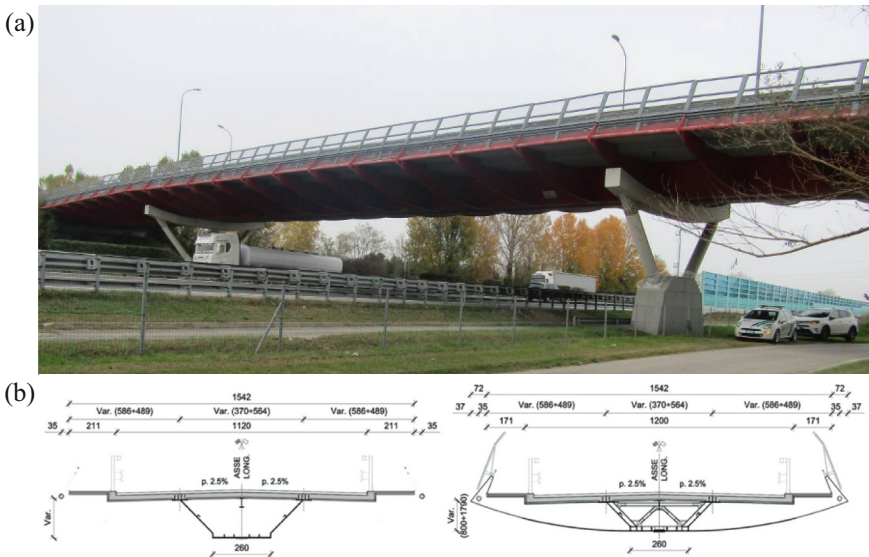


Fig. 1. View (a) and transversal cross-sections (b) of the *Dolo* overpass (dimensions in cm).

3 Preliminary Ambient Vibration Tests and FE Modeling

In order to properly design a dynamic monitoring system, prior knowledge of the modal parameters of the structure is generally required. Hence, the investigated overpass underwent to preliminary ambient vibration tests (AVTs), that were performed on 10–11

November 2020. The response of the bridge was measured at 22 selected points (Fig. 2) that were also permanently instrumented during the subsequent dynamic monitoring. Since 14 accelerometers were available during the tests, 2 set-ups were performed to measure the acceleration responses at the opposite sides of the deck, considering 4 sensors (placed at the opposite sides of two reference cross sections) as reference transducers, which were kept at the same locations in the two set-ups.

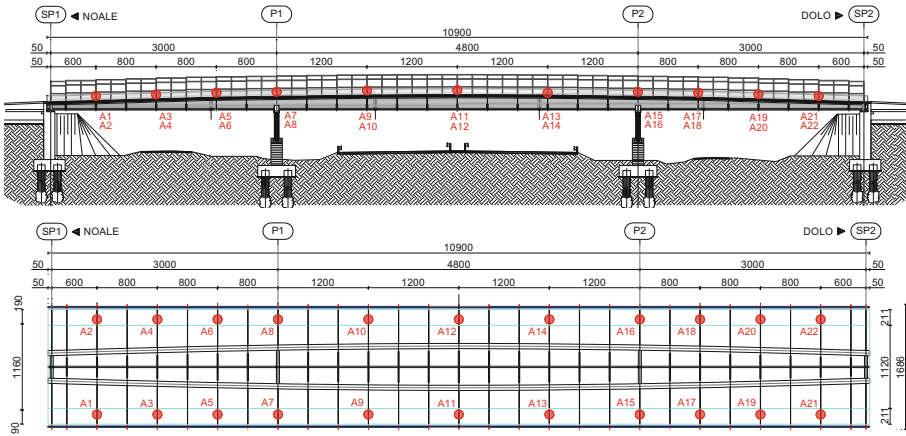


Fig. 2. Elevation and plan of the *Dolo* overpass (dimensions in cm) and schematic of the sensor layout during the preliminary AVT and the continuous monitoring.

Time series of 3600 s were recorded in each set-up at a sampling rate of 200 Hz, which is much higher than that required for this bridge, as the natural frequencies of the dominant modes are below 10 Hz (Fig. 3). Hence, low pass filtering and decimation were applied to the data before the use of the identification tools [11], reducing the sampling rate from 200 Hz to 20 Hz. The extraction of modal parameters from ambient vibration data was carried out by using the covariance-driven Stochastic Subspace Identification (SSI-Cov) algorithm [12] and 7 vibration modes were identified in the frequency range of 0–6 Hz: as shown in Fig. 3, the observed modes can be arranged as vertical bending modes (B) and vertical torsion (T) modes of the deck.

A 3D FE model of the bridge was developed by using the MIDAS Civil software [13] to complement the preliminary tests. The numerical model includes the 3-span steel-concrete composite deck and the steel elements of the intermediate piers (Figs. 4 and 5); it consists of 12376 finite elements (3980 beam elements and 8396 shell elements, with in-plane and out-of-plane stiffness) and the total number of nodes is equal to 9857.

As shown in Figs. 4 and 5, the steel-concrete composite deck modelling includes: (a) the longitudinal steel box-girder and its stiffeners, (b) the steel cross-beams at the abutments and piers, (c) the steel floor beams that are equally spaced along the bridge spans, (d) the steel bracing system and (e) the reinforced concrete deck. The steel pier modelling includes the two pairs of inclined legs and the top beam underneath the transverse beams of the deck.

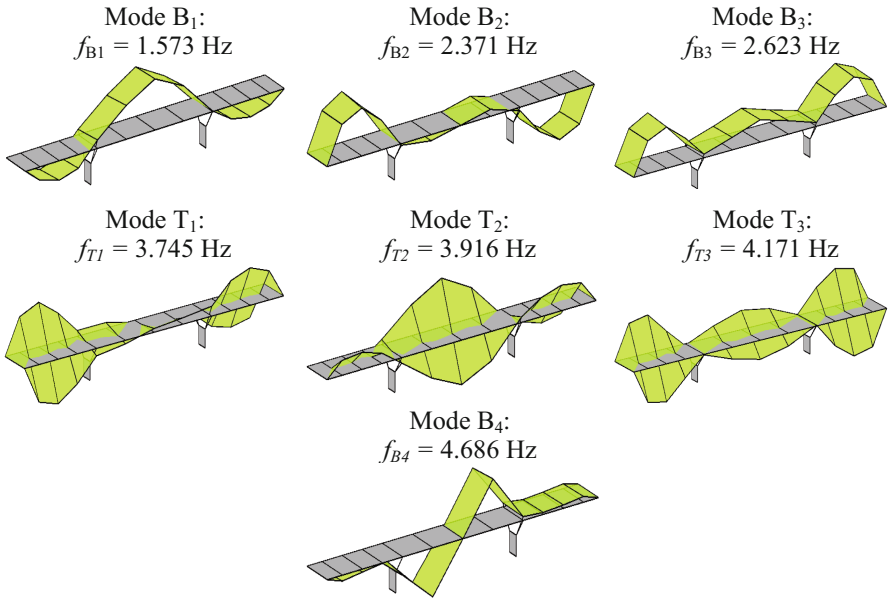


Fig. 3. Reference modes identified (SSI-Cov) in the AVT of November 2020.

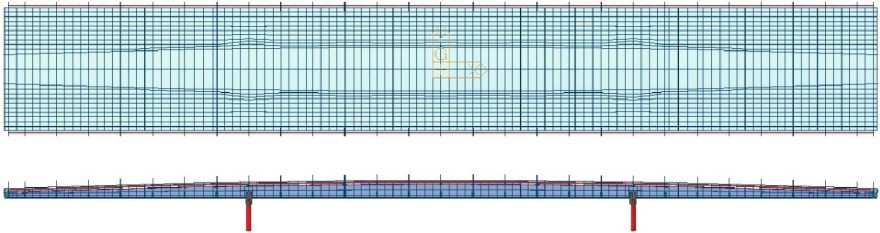


Fig. 4. Top and lateral views of the 3D FE model.

The steel members were modelled using either beam elements or 3-node/4-node shell elements, whereas 4-node shell elements were used to model the concrete deck.

The elastic properties of the structural members were assigned according to the S355 steel grade, and the C40/50 concrete grade as provided by the relevant Eurocodes. Consequently, the following values of Young's modulus and Poisson's ratio were assumed for steel and concrete: (a) steel, $E_s = 210$ GPa and $\nu_s = 0.3$; (b) concrete, $E_c = 35.20$ GPa and $\nu_c = 0.2$.

The resonant frequencies associated to the vibration modes estimated from the FE model are similar to the ones obtained during the AVT of November 2020 (Fig. 6), since their differences range from 0.1 to 1.9%.

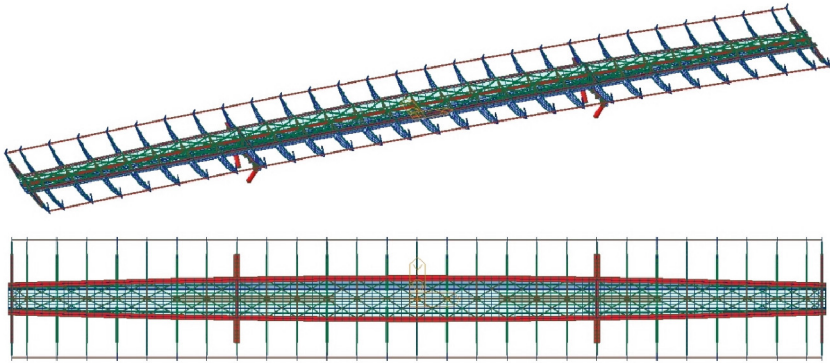


Fig. 5. 3D and plan views of the bridge deck model.

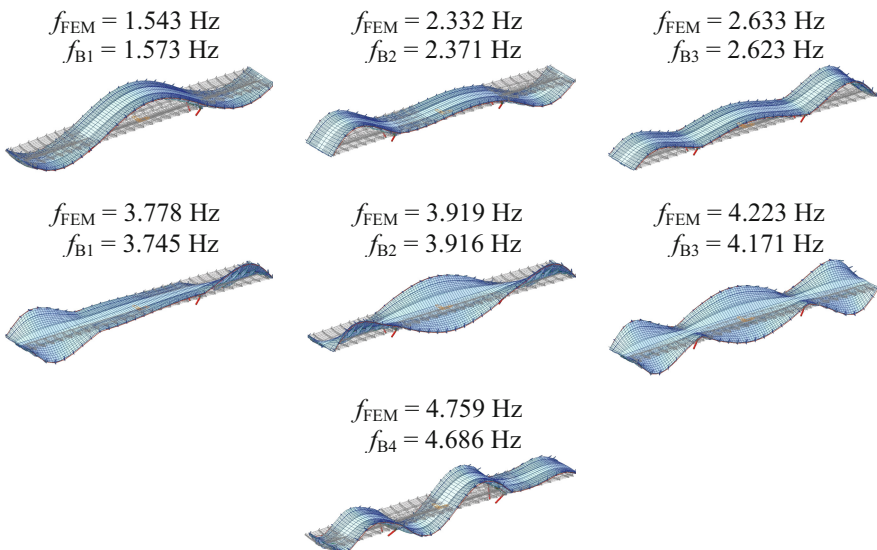


Fig. 6. Comparison between the natural frequencies obtained from the FE model and the experimental ones (AVT, November 2020).

4 Continuous Dynamic Monitoring and Results

After the preliminary AVTs performed in November 2020, a dynamic monitoring system has been installed on the bridge. The monitoring system is active since the second half of January 2022 and includes 22 MEMS accelerometers (Fig. 2) and 1 temperature sensor. The acceleration data are recorded at a sampling rate of 125 Hz and the length of time windows used for the modal parameters estimation (MPE) was set equal to 3600 s (1 h). In the first year of monitoring (from 23 January 2022 to 22 January 2023), 8760 datasets have been collected and processed.

The MPE and the modal tracking (MT) have been automatically performed by applying the MATLAB software package developed in [11] and called DYMOND. The SSI-Cov algorithm [12] and the procedure have been adopted for automated MPE and MT, respectively.

Since especially the variation of natural frequencies is affected by EOV, the Cointegration technique [8, 9] is used to create an appropriate linear combination of the identified frequencies, namely the cointegration residual, with this latter function being purged from the trends determined by EOV. The parameters of the linear combination are determined through the Johansen procedure [8], which is a maximum-likelihood multivariate technique employing the investigated features (i.e., the natural frequencies) to construct a cointegrating relationship within a training period: the cointegration residual is therefore a new time series in which the common trends present in the original features have been removed. Consequently, the occurrence of a structural anomaly is identified when the cointegration residual exceeds the threshold defined during the training period.

4.1 Results

Since the first weeks of monitoring, the time evolution of the automatically identified frequencies clearly shows daily oscillations that are conceivably due to temperature variation. Furthermore, the influence of temperature is clearly confirmed by the inspection of Fig. 7, illustrating the time evolution of the identified frequencies (Fig. 7a) and the measured air temperature (Fig. 7b) during the first year of monitoring (i.e., from 23 January 2022 to 22 January 2023). More specifically, the long-term (seasonal) variation of natural frequencies is clearly detected in Fig. 7: as expected, all natural frequencies decrease with increased temperature.

The variation in time of the frequencies of both bending and torsion modes is better exemplified in Figs. 8 (mode B_1) and 9 (mode T_2), along with the frequency-temperature correlation: it should be observed that the correlation with temperature is characterized by high coefficient of determination R^2 (0.739 for mode B_1 and 0.906 for mode T_2), clearly indicating that temperature turns out to be the dominant driver of frequency changes. It is also worth noticing that R^2 range between 0.53 and 0.98 (Table 1) for the frequencies identified in the first year of monitoring.

Table 2 summarizes the mean value (f_{mean}) and the standard deviation (σ_f) of the frequency estimates, the extreme values ($f_{\text{min}}, f_{\text{max}}$) of each frequency as well as the mean and minimum value of the MAC and the identification rate.

The inspection of the results summarized in Figs. 7, 8 and 9 seems to indicate that the variation of natural frequencies is mostly arising from normal temperature changes. In addition, the linear dependencies exhibited by the monitored natural frequencies (Table 1) suggests the use of the linear Cointegration technique [8, 9] to verify that no structural anomaly occurs. Hence, the parameters of the linear combination are determined by applying the Johansen procedure [8] to first 8 months of monitoring (i.e., from 23 January 2022 to 22 October 2022) in order to use the stationarity of the cointegration residual as indicator of structural degradation, by means of a control chart. The confidence interval was set at 99% within the training period (Fig. 10).

Table 1. Determination coefficients between the natural frequencies identified from 23/01/2022 to 22/01/2023.

R^2	f_{B1}	f_{B2}	f_{B3}	f_{T1}	f_{T2}	f_{T3}	f_{B4}
f_{B1}	1	0.856	0.844	0.900	0.881	0.881	0.761
f_{B2}	–	1	0.767	0.763	0.722	0.735	0.631
f_{B3}	–	–	1	0.721	0.650	0.655	0.528
f_{T1}	–	–	–	1	0.923	0.926	0.865
f_{T2}	–	–	–	–	1	0.978	0.899
f_{T3}	–	–	–	–	–	1	0.905
f_{B4}	–	–	–	–	–	–	1

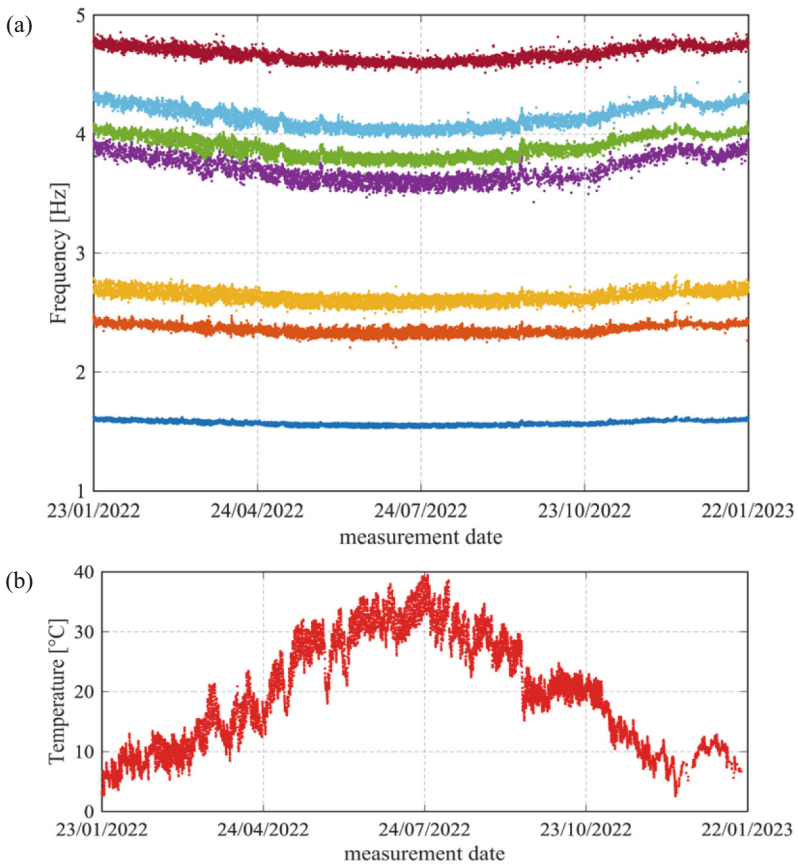


Fig. 7. Time evolution of identified natural frequencies (a) and measured temperature (b) from 23/01/2022 to 22/01/2023.

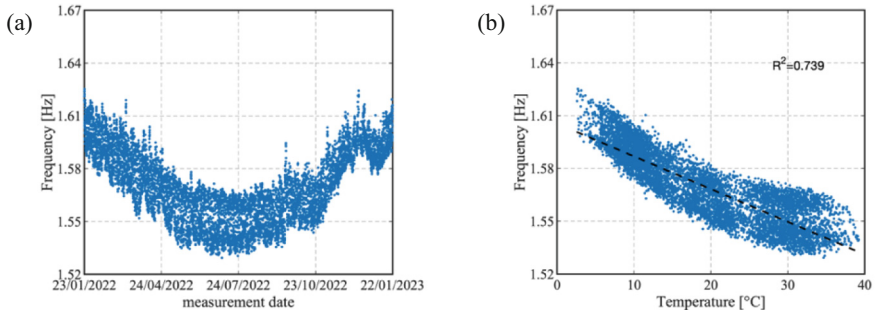


Fig. 8. Mode B₁: evolution of natural frequency (a) and temperature-frequency correlation (b).

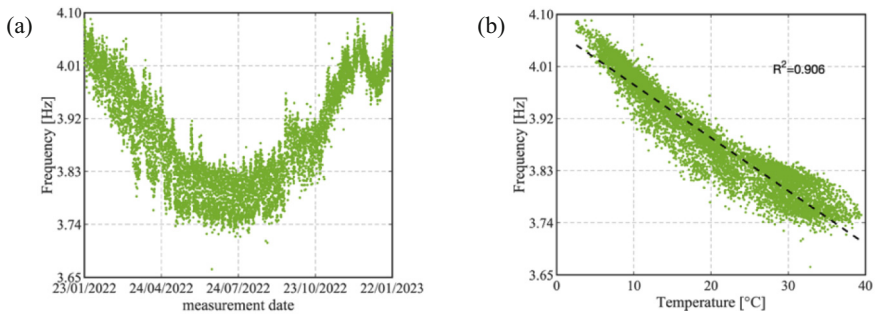


Fig. 9. Mode T₂: evolution of natural frequency (a) and temperature-frequency correlation (b).

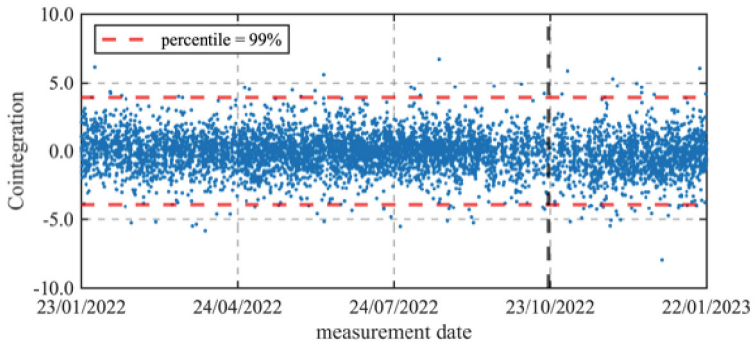


Fig. 10. Time evolution of Cointegration residual from 23/01/2022 to 22/01/2023.

Figure 10 shows that, starting from the training period, the residual remains stationary, with negligible occurrence of outliers, suggesting the absence of any appreciable structural anomalies in the investigated time period.

As previously pointed out, the evolution of mode shapes is checked by means of the MAC (Figs. 11 and 12).

Figure 11 refers to bending modes B_1 - B_2 and shows a clear increase of MAC dispersion between September and November 2022: this anomaly was due to a temporary electrical malfunction, generating the worsening of the signal-to-noise ratio in the collected signals. On the other hand, the electrical malfunction was solved in the second part of November 2022 and the MACs returned close to unitary values.

Unlike bending modes, that are not significantly affected by EOv, torsion modes reveal a clear pattern due to thermal variation: as shown in Fig. 12, towards the hot season, the MAC value decreases. This uncommon phenomenon is conceivably related to the elastic torsion constraints between deck and piers (see Fig. 1). Anyway, also for torsion modes, the MAC returns back to 0.9–1.0 after the hot season.

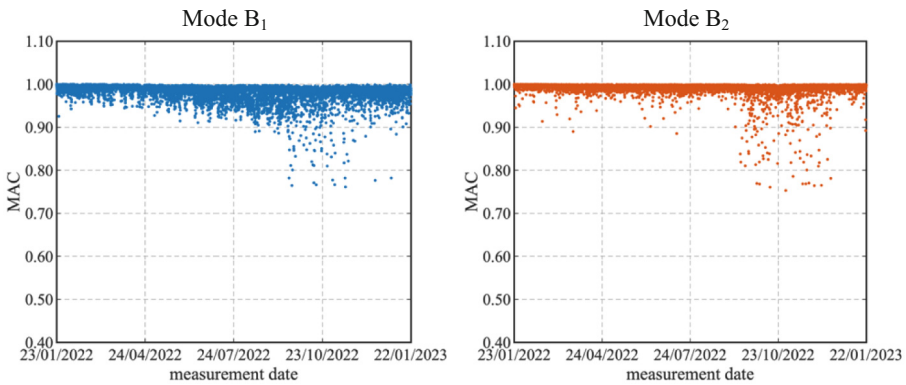


Fig. 11. Bending vibration modes: evolution of MAC from 23/01/2022 to 22/01/2023.

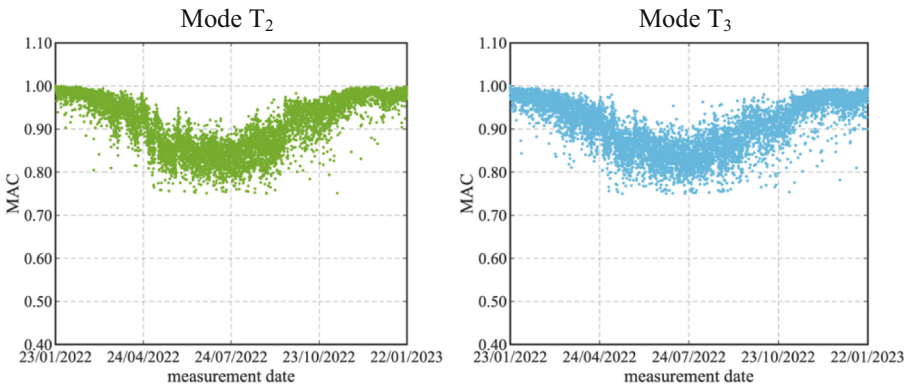


Fig. 12. Torsion vibration modes: evolution of MAC from 23/01/2022 to 22/01/2023.

Table 2. Statistics of the modal parameters identified from 23/01/2022 to 22/01/2023.

Mode Id:	f_{mean} (Hz)	σ_f (Hz)	f_{min} (Hz)	f_{max} (Hz)	MAC _{mean}	MAC _{min}	Id.Rate (%)
B ₁	1.571	0.020	1.529	1.625	0.980	0.761	86.9
B ₂	2.356	0.039	2.251	2.507	0.991	0.753	93.4
B ₃	2.628	0.050	2.490	2.811	0.985	0.750	93.0
T ₁	3.694	0.111	3.469	4.009	0.950	0.751	57.2
T ₂	3.893	0.093	3.709	4.100	0.914	0.750	90.3
T ₃	4.141	0.096	3.961	4.393	0.906	0.750	83.7
B ₄	4.668	0.061	4.516	4.845	0.989	0.758	90.2

5 Conclusions

The paper illustrates the OMA-based strategy adopted for the SHM of a steel-concrete composite overpass. Preliminary investigations, FE modelling and the results collected in the first year of monitoring allowed the following main conclusions:

1. Within the frequency range 0–6 Hz, 7 vibration modes were successfully identified in preliminary AVTs as well as during continuous monitoring.
2. A 3D FE model was developed and showed fairly good correlation with the experimental results.
3. The air temperature turned out to be a dominant driver of the daily and seasonal fluctuation of the natural frequencies of all modes.
4. The linear Cointegration approach is used to purge from the common trends due to EOVS environmental and operational variability and to create a damage-sensitive feature. The control chart based on the cointegration residual has not shown any structural change in the investigated monitoring period.

References

1. Wenzel, H.: Health Monitoring of Bridges. John Wiley & Sons (2009)
2. Peeters, B., De Roeck, G.: One-year monitoring of the Z24-bridge: environmental effects versus damage events. *Earthq. Eng. Struct. D* **30**, 149–171 (2001)
3. Magalhães, F., Cunha, A., Caetano, E.: Vibration based structural health monitoring of an arch bridge: from automated OMA to damage detection. *Mech. Syst. Signal.* **28**, 212–228 (2012)
4. Cross, E.J., Koo, K.Y., Brownjohn, J.M.W., Worden, K.: Long-term monitoring and data analysis of the Tamar Bridge. *Mech. Syst. Signal Process.* **35**(1–2), 16–34 (2013)
5. Gentile, C., Saisi, A.: Continuous dynamic monitoring of a centenary iron bridge for structural modification assessment. *Front. Struct. Civ. Eng.* **9**(1), 26–41 (2014). <https://doi.org/10.1007/s11709-014-0284-4>
6. Borlenghi, P., Gentile, C., Pirrò, M.: Continuous dynamic monitoring and automated modal identification of an arch bridge. In: Rizzo, P., Milazzo, A. (eds.) *European Workshop on Structural Health Monitoring. EWSHM 2022. LNCE*, vol. 254. Springer, Cham (2022). https://doi.org/10.1007/978-3-031-07258-1_18

7. Farrar, C.R., Worden, K.: An introduction to structural health monitoring. *Philos. Trans. R Soc. Math. Phys. Eng. Sci.* **365**(1851), 303–315 (2007)
8. Johansen, S.: Statistical analysis of cointegration vectors. *J. Econ. Dyn. Control.* **12**(2–3), 231–254 (1988)
9. Cross, E., Worden, K., Chen, Q.: Cointegration: a novel approach for the removal of environmental trends in structural health monitoring data. *Proc. R. Soc. A* **467**, 2712–2732 (2011)
10. Allemang, R.J., Brown, D.L.: A correlation coefficient for modal vector analysis. In: *Proceedings 1st International Modal Analysis Conference* (1982)
11. Pirrò, M.: Automated operational modal analysis and tracking: development of software tools and applications. M.Sc. thesis, Politecnico di Milano, Italy (2021)
12. Peeters, B., De Roeck, G.: Reference-based stochastic subspace identification for output-only modal analysis. *Mech. Syst. Signal. Process* **13**(6), 855–878 (1999)
13. MIDAS Civil 2022 (v1.2), MIDAS Information Technology Ltd., Korea
14. Cabboi, A., Magalhães, F., Gentile, C., Cunha, À.: Automated modal identification and tracking : application to an iron arch bridge. *Struct. Control. Health Monit.* **24**(1), e1854 (2017)